HHS Public Access

Author manuscript

Anal Chem. Author manuscript; available in PMC 2022 October 18.

Published in final edited form as:

Anal Chem. 2022 January 18; 94(2): 1011–1021. doi:10.1021/acs.analchem.1c03960.

Isothermal Amplification with a Target-Mimicking Internal Control and Quantitative Lateral Flow Readout for Rapid HIV Viral Load Testing in Low-Resource Settings

Ian T. Hull[1],

Enos C. Kline[1],

Gaurav K. Gulati[1],

Jack Henry Kotnik[1],

Nuttada Panpradist[1],

Kamal G. Shah[1],

Qin Wang[1],

Lisa Frenkel[2,3,4,6],

James Lai[1],

Joanne Stekler[5],

Barry R. Lutz[1,*]

[1]Department of Bioengineering, University of Washington, Seattle, WA 98195-5061, USA

[2]Department of Pediatrics, University of Washington, Seattle, WA 98195-9300, USA

[3]Department of Laboratory Medicine and Pathology, University of Washington, Seattle, WA 98195-7470, USA

[4]Department of Global Health, University of Washington, Seattle, WA 98195-1620, USA

[5]Department of Medicine, University of Washington, Seattle, WA 98195-6420, USA

[6]Center for Global Infectious Disease Research, Seattle Children's Research Institute, Seattle, WA 98145-5005, USA

Abstract

Point-of-care diagnostics often use isothermal nucleic acid amplification for qualitative detection of pathogens in low-resource healthcare settings, but lack sufficient precision for quantitative applications such as HIV viral load monitoring. Although viral load monitoring is an essential component of HIV treatment, commercially available tests rely on relatively high-resource chemistries like real-time polymerase chain reaction and are thus used on an infrequent basis for millions of people living with HIV in low-income countries. To address the constraints

*Send correspondence to blutz@uw.edu.

Author Contributions

I.T.H. designed the competitive RPA workflow, conducted all assays, and analyzed lateral flow results. E.C.K. contributed to competitive isothermal assay design. G.K.G. prepared RNA from HIV-positive plasma samples. J.H.K. and N.P. conducted the survey for naked-eye analysis of lateral flow strips. K.G.S. developed the MATLAB script for analysis of cell phone photos of lateral flow strips and Q.W. conducted the cell phone analysis. L.F. and J.S. contributed analysis of the clinical utility of this work. J.L. and B.R.L. oversaw the study. All authors contributed to writing and/or review of this manuscript.

of low-resource settings on nucleic acid quantification, we describe a recombinase polymerase amplification and lateral flow detection approach that quantifies HIV-1 DNA or RNA by comparison to a competitive internal amplification control (IAC) of known copy number, which may be set to any useful threshold (in our case, a clinically relevant threshold for HIV treatment failure). The IAC is designed to amplify alongside the HIV target with similar efficiency, allowing normalization of the assay to variation or inhibition, and enabling an endpoint readout that is compatible with commercially available kits for nucleic acid lateral flow detection and interpretable with minimal instrumentation or by naked eye. We find that this approach can reliably differentiate ≤600 or ≥1400 copies of HIV DNA from a 1000-copy threshold when lateral flow strips are imaged with a conventional office scanner and analyzed with free densitometry software. We further demonstrate a user-friendly adaptation of this analysis to process cell phone photos with an automated script. Alternatively, we show via survey that 21 minimally trained volunteers could reliably resolve ≥10-fold (log_{10}) differences of HIV DNA or RNA by naked-eye interpretation of lateral flow results. This amplification and detection workflow requires minimal instrumentation, takes just 30 minutes to complete, and when combined with a suitable sample preparation method, may enable HIV viral load testing while the patient waits or a self-test, which has the potential to improve care. This approach may be adapted for other applications that require quantitative analysis of a nucleic acid target in low-resource settings.

For Table of Contents Only

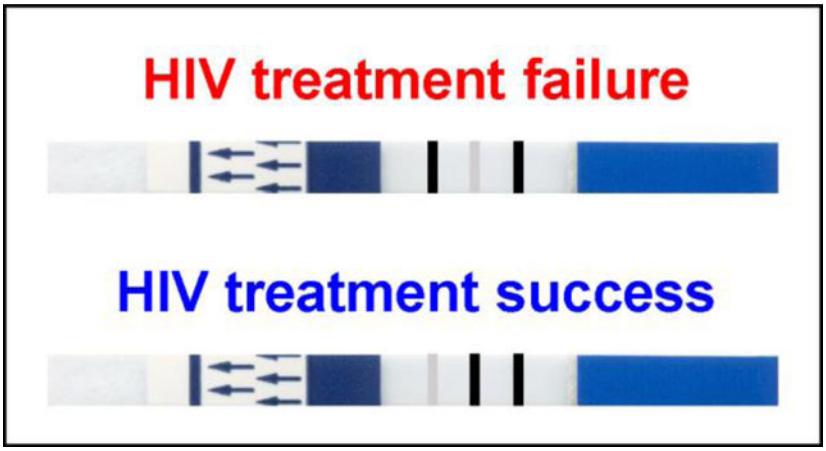

Introduction

Isothermal nucleic acid tests (NATs) are useful for point-of-care (POC) diagnostics due to their minimal requirements for instrumentation and user expertise. Unlike polymerase chain reaction (PCR), isothermal reactions amplify nucleic acids at a constant temperature and do not require a specialized thermal cycler, enabling POC detection of pathogens[1,2]. Quantitative applications of isothermal amplification, however, are difficult to implement at POC. Most quantitative NATs rely on real-time PCR to quantify a target based on number of cycles needed for the signal to exceed a certain threshold, as endpoint signal typically plateaus regardless of input copy number[3]. Real-time analysis requires fluorescence readers and external quantitative standards, which increase assay complexity. Isothermal techniques

carry additional complications for real-time analysis, as the lack of thermal cycling to regulate amplification makes liftoff time highly sensitive to variations in reaction conditions such as incubation temperature[4], mixing[5], or interfering substances.

As a result, real-time PCR remains the standard technique for the most impactful quantitative NAT in global public health: HIV viral load (VL) monitoring. VL monitoring is integral to the management of antiretroviral therapy (ART). The VL of a person living with HIV (PWH), expressed as the number of HIV RNA copies per milliliter (c/mL) of plasma, is measured frequently during ART to monitor suppression of HIV replication. A VL that remains above 1000c/mL is defined as virologic failure by the World Health Organization (WHO) and is associated with HIV transmission and drug resistance. Persistent failure leads to depletion of CD4+ T cells and progression to AIDS[6]. Other public health authorities use lower VL thresholds (e.g. ≥200c/mL) to define virologic failure[7]. Virologic failure, or really any lack of virologic suppression, warrants clinicians to discuss medication adherence and potentially to evaluate virus for drug resistance.

Although roughly 32 of 37 million PWH globally reside in low- to middle-income countries (LMIC)[8], VL monitoring typically relies on high-resource tests that require expensive equipment and centralized laboratory facilities[9] such as real-time PCR by COBAS® Taqman® v2.0 (Roche) or the RealTi*m*e HIV-1 (Abbott). As a result, less than half of PWH on ART globally received routine (annual) VL tests in 2016[10] (with access particularly low in sub-Saharan Africa, at 37% in Eastern and Southern Africa and 13% in Western and Central Africa[11]).

For quantitative NATs to have an impact in global public health, the constraints of POC settings must be addressed. An ideal POC HIV VL test, for example, requires minimal (ideally battery-powered) instrumentation, results within 30 minutes, resolution within 0.3 $\log_{10}$ (~2-fold) copies RNA, and sensitivity sufficient for fingerstick blood volumes (≤200μL)[12]. One assay developed by Crannell *et al.* uses real-time recombinase polymerase amplification (RPA)[13], which is an adaptation of a qualitative lateral flow RPA assay originally described by Boyle *et al.*[14]. This approach is isothermal, fast (< 30 minutes), and accurate to within 0.3 $\log_{10}$ copies of DNA for most inputs. However, it relies on real-time analysis, increasing assay complexity and vulnerability to errors due to reaction inhibition. Nycz *et al.* described a strand-displacement amplification (SDA) assay with a target-mimicking internal amplification control (IAC)[15]. This approach is endpoint-based and controls for reaction variability, saturation, and inhibition by comparing the HIV signal to that of the IAC, which co-amplifies at a fixed ratio dependent on the initial ratio of HIV and IAC input. This “competitive” approach is accurate and effective; in fact, competitive PCR predates real-time PCR and was the original technique used to establish the relationship between HIV VL and progression to AIDS early in the HIV/AIDS pandemic[16]. Nycz *et al.*[15] expanded this concept to an isothermal chemistry, but used radiolabeled probes and an electrophoresis readout that would be inaccessible in POC settings.

Here, we describe an isothermal quantitative or semi-quantitative NAT with features accessible in POC settings. We combine the HIV RPA assay described previously with the competitive IAC quantification approach previously used in PCR and SDA. By comparing

amplification of the HIV target relative to the IAC, we establish that the resulting fractions in endpoint signal can be used semi-quantitatively to determine if the HIV input exceeds the IAC threshold (which should be sufficient for most POC VL tests), or quantitatively to estimate HIV input copy number with 95% confidence intervals (which may be used for tracking of ART efficacy over time). This “competitive RPA” assay has several advantages. Analysis occurs at endpoint, minimizing instrumentation and enabling a lateral-flow-strip readout that can be interpreted by the naked eye or automated with a commercially available cell phone camera. The competitive IAC enhances the accuracy of the assay and accounts for inhibiting conditions by normalizing HIV amplification relative to that of the IAC. Finally, we show that the assay maintains accuracy when challenged with common HIV-1 genomic variants. Given these qualities, this competitive amplification approach should prove to be a useful template to develop various isothermal quantitative NATs, including but not limited to POC HIV VL tests.

Experimental Section

RPA Primer, Probe, and Synthetic Template Designs

We chose the HIV *pol* RPA assay described by Boyle *et al.*[14] for modification to include a competitive IAC and biplexed lateral flow detection of HIV and IAC targets. The primer designs and HIV probe sequence are unchanged from the original *pol* assay[14], but the HIV probe was given a 5’ digoxigenin label for lateral flow detection. The IAC probe sequence was designed using Geneious 11.1.4 (https://www.geneious.com) to comprise the same base content as the HIV probe, but with a shuffled sequence. The Mutate & Shuffle plugin was used to randomize the positions of all bases in the IAC probe except the “TGC_CT” motif at positions 28–33. This motif was preserved so that the endonuclease IV probe system would have similar kinetics at the abasic site and so the flanking thymidines could be used as conjugation sites for alternative fluorescence-based probe chemistries (not shown). We used the DNA Fold tool in Geneious to screen 20 shuffled probe sequences *in silico* for predicted secondary structure at 39°C. We chose the sequence with minimal secondary structure for use in the IAC probe and gave this probe a 5’ 6-FAM label for lateral flow detection. Synthetic templates were based on sequences from the Los Alamos National Laboratory (LANL) HIV Sequence Database[17]; all experiments used a majority consensus sequence HIV-1 template (unless otherwise noted) and an IAC template identical to the HIV template except with IAC probe sequence substituted at the probe site. Finally, each template was given flanking PCR primer sites and a T7 promoter site to enable in-house DNA and RNA production. Full template design notes are included in the Supplementary Information. All primer, probe, and template DNA sequences were ordered from Integrated DNA Technologies (IDT) (Coralville, Iowa) and are listed in Table S1.

Synthetic Template Preparation and Quality Control

To better quantify DNA templates prior to use in our assay, we amplified our gBlocks using M13 PCR primers and Q5 HotStart High-Fidelity DNA Polymerase (New England BioLabs (NEB) M0493). Each 50μL PCR reaction contained 1x Q5 Reaction Buffer, 200μM each dNTPs, 500nM each M13 primer, 1U Q5 HotStart High-Fidelity DNA Polymerase, and 10ng gBlock template. PCR thermal cycling parameters were: 98°C for 30 seconds, 25

cycles of [98°C for 5 seconds, 57°C for 10 seconds, 72°C for 5 seconds], then 72°C for 2 minutes. PCR amplicons were purified using a QIAquick PCR Purification Kit (Qiagen 28104) or PureLink PCR Purification Kit (Invitrogen K310002). PCR amplicons were then quantified using a ThermoFisher NanoDrop 2000c and stored in aliquots of 10^9 copies dsDNA template per µL.

To prepare synthetic RNA templates, we transcribed the dsDNA PCR amplicons using T7 RNA Polymerase (NEB M0251S) using the manufacturer-recommended protocol and 100ng of template DNA. RNA transcripts were purified using a Monarch RNA Cleanup Kit (NEB T2030), checked for length and integrity using an RNA ScreenTape Assay (Agilent 5067–5576) on a TapeStation 2200, and quantified with a Qubit High-Sensitivity RNA Assay (ThermoFisher Q32852). The RNA was then diluted with nuclease-free water to 10^9 copies/µL and stored at −80°C in single-use 50µL aliquots.

RPA nfo Reactions

RPA nfo reactions (TwistDx TANFO02KIT (temporarily discontinued)) were set up as recommended by the manufacturer. Briefly, a master mix was prepared such that the 50µL reactions would have final concentrations of 1x primer-free rehydration buffer, 420nM each primer, and 60nM each probe. For reactions with RNA templates, the master mix was supplemented such that each 50µL reaction would contain 4U OmniScript Reverse Transcriptase (Qiagen 205111) and 50U human pancreatic ribonuclease inhibitor (NEB M0307). Lyophilized RPA nfo pellets were resuspended with 45.5µL of master mix. A 2.5µL droplet of 280mM magnesium acetate was added to the lid of each reaction tube. Finally, 2µL of template were added to each reaction tube.

Reactions were initiated by spinning the magnesium acetate droplets down into reactions using a microcentrifuge, vortexing briefly, and spinning down once more. Reactions were then immediately transferred to a preheated Bio-Rad T100 thermal cycler. All reactions were incubated at 39° for 20 minutes unless otherwise noted. 5 minutes into incubation, the thermal cycler timer was paused and reactions were briefly mixed via vortex and spun down before being returned to the thermal cycler to resume incubation. At the end of incubation, reactions were rapidly cooled to 4°C on the thermal cycler, spiked with 5µL each of 0.5M EDTA to stop amplification, vortexed briefly, and spun down. The amplicons were then run immediately on lateral flow strips or stored overnight at 4°C before continuing with lateral flow detection.

Lateral Flow Detection of RPA nfo Amplicons

Lateral flow assays were performed using PCRD-FLEX strips (Pocket Diagnostics FD51676) in a 96-well plate on an open benchtop. Unless otherwise noted, 1µL of RPA nfo amplicons was mixed with 149µL of PCRD extraction buffer in a single well of the 96-well plate. (See Figure S2 for our justification to use 1µL of amplicons instead of the recommended 10µL). One PCRD-FLEX strip was dipped into each well and allowed to wick for 10 minutes.

PCRD-FLEX strips were then removed from the wells and taped to a sheet of printer paper. The strips were scanned within 15 minutes using an Epson Perfection V700 photo scanner

and SilverFast Software SE 8.5 (LaserSoft Imaging). All strips from each experiment were scanned as a single image. Raw images were saved in TIF format at a resolution of 600 pixels per inch.

For some experiments as noted, the strips were then allowed to dry completely (to reduce artifacts from refractive index dependent on membrane wetness) and individually photographed using an iPhone 11 camera using default settings and 1x zoom via the Camera application. Strips were photographed under weak ambient laboratory lighting, with care taken to avoid strong and/or directional lighting sources, as these may cause overexposure or lighting gradients in the photos.

Analysis of Lateral Flow Capture Line Intensities

Scanner-Based Imaging and Analysis—All software-based analyses of the strips were conducted with scanned images except those labeled as cell phone analysis. Scanned images of the lateral flow strips were processed in Image Studio Lite Version 5.2 (LI-COR, discontinued). Boxes of equal dimensions (within each experiment) were drawn around each capture line, excluding the edges of lateral flow strips to eliminate flow artifacts and shadows. The background for each box was specified as the median of all green-channel intensities 3 pixels above or below the box. The raw signal for each capture line was determined by subtracting the background of its box from the green-channel intensities of each pixel within the box and summing across all pixels within the box. The HIV and IAC signals for each strip were further normalized relative to each other, such that for each strip, the “HIV signal fraction” equals (DIG/(DIG+FAM)) and the “IAC signal fraction” equals (FAM/(DIG+FAM)).

The intended assay format, in which a known quantity of IAC target is co-amplified with an unknown quantity of HIV, should always produce a signal in one or both capture lines, as IAC is present even when HIV is undetectable. If neither line is observed, it should be interpreted clinically as a failed or inconclusive reaction, from which no information can be drawn. Such failed reactions could have multiple causes, including reagent expiry, inputs below the assay limit of detection, improper amplification conditions, or inhibition due to contaminants. These reactions should not be used for diagnosis or quantification because the capture line intensities are dominated by random noise. To identify such reactions, we chose a cutoff for minimum capture line intensity that indicates a successful amplification and can be used for quantification. Reactions were classified as “failed” if the raw DIG and FAM signals were both less than 12,000 units despite a positive HIV and/or IAC input. This cutoff was chosen retroactively, as we observed that the noise of raw DIG or FAM signals from reactions without their respective targets fell within a range of ±8,000 across all experiments, but a cutoff of +12,000 was necessary to minimize divide-by-zero errors from strips with very faint (i.e. noisy) capture lines. All failed reactions are labeled with an ‘X’ in strip images and omitted from plots where noted. FC lines were visible (and well above the 12,000-unit cutoff) for all reactions; therefore, we attribute failed reactions to insufficiently sensitive amplification, rather than any problems with the lateral flow assays. Note that all “NTC” reactions (to which we added neither IAC nor HIV) also had raw DIG and FAM signals below the 12,000-unit cutoff and would be classified as “failed” in a real-world

context (e.g. if sample preparation failed and no HIV or IAC was added to the reaction), but for clarity, we distinguish here between NTCs and reactions that fail despite a positive input.

Cell-Phone-Based Imaging and Analysis—Images of the lateral flow strips taken by iPhone 11 camera were processed using an in-house automated script using MATLAB[18] (code provided in supplement). Briefly, this script imported cell phone images and cropped to nitrocellulose membranes of individual lateral flow strips (using blue regions of the PCRD FLEX strips as a reference). It then obtained a signal profile of each strip for the centermost 50% of the width and 90% of the length of the nitrocellulose membrane. This signal profile was first integrated across the width of the strip, then saved with respect to the length. The user manually designates certain positive strips as a reference for the location of the three capture lines in each strip. Finally, the script determines the area under the curve of signal at the three capture lines for each strip.

Non-Linear Regression Analysis—Where noted, mathematical curves describing the relationship between HIV input copy number and HIV signal fraction were determined using non-linear regression analysis in GraphPad Prism version 9.2.0 for Windows (GraphPad Software). We fit four-parameter logistic curves (“Sigmoidal, 4PL, X is concentration”) to data using least squares regression (all default options). All analyses passed the D’Agostino-Pearson omnibus (K2) test[19] to verify that data was normally scattered around the curves. Curves and 95% prediction bands are included as plots in figures; parameters defining these curves and other results of non-linear regression analysis are available in Table S2.

Naked-Eye-Based Analysis—Scanned images of lateral flow strips were cropped to contain only the nitrocellulose membrane from one strip per image. They were then digitally annotated with a random, unique numerical identifier and three arrows, each indicating the position of an expected test line (typical lateral flow cartridges for consumer use similarly indicate these positions). Images were assigned a random order and copied into a survey instrument (Google Forms, forms.google.com) (Figure S3). Volunteers were recruited from “non-lab” (N = 14) and “lab” personnel (N = 7) familiar with lateral flow assays but blinded to the inputs of each strip. Volunteers were given a short description of the test’s purpose and function, and a schematic showing the different possible outcomes of the test, with a letter A-G and a short description (Figure S3). The answers in the survey corresponded to the A-G outcomes on the schema; volunteers completed the survey using the schematic as a guide. Images were annotated using ImageJ (https://imagej.nih.gov/ij/)[20]. This study was approved by the University of Washington Human Subjects Division (IRB STUDY00013312).

Results and Discussion

Designed Competitive IAC Mimics HIV Target by using Identical Primer Sites and Shuffled Probe Sequence

We designed a competitive IAC (Figure 1) to incorporate into the HIV-1 RPA assay described by Boyle et al.[14]. Design of the IAC to mimic the HIV target as closely as possible was essential, as the quantitative nature of the competitive amplification depends on

identical amplification efficiency for both targets. Isothermal amplification of a target can be roughly modeled as exponential growth:

$$HIV(t) = HIV_{t=0} \cdot 2^{\frac{t}{\tau_{HIV}}}$$
$$IAC(t) = IAC_{t=0} \cdot 2^{\frac{t}{\tau_{IAC}}}$$

where t represents time since reaction initiation and τ represents the doubling time (a representation of amplification efficiency) for a specific target. If both targets possess equal amplification efficiency, then $\tau_{HIV} = \tau_{IAC}$ and the endpoint ratio ($\frac{HIV(t)}{IAC(t)}$) will equal the input ratio ($\frac{HIV_{t=0}}{IAC_{t=0}}$). However, slight differences in amplification efficiency can lead to large deviations from the input ratio; for example, if $\tau_{HIV} = 60s$ and $\tau_{IAC} = 57s$, then the IAC yield will be roughly double the HIV yield after 20 minutes, and VL will be underestimated. This simplified model does not capture more complicated phenomena, such as reagent diffusion and depletion[21], but illustrates the importance of preserving amplification efficiency for this application, particularly because isothermal amplification lacks thermal cycling to synchronize doubling times.

Amplification efficiency is influenced by many factors, including primer sequence, target sequence, target length, and GC content[22]. To control these factors, we made the minimum modification necessary to achieve specific probe binding to the IAC, by shuffling bases at the probe site yet preserving overall target length, base content, and non-probe sequence. The competitive IAC is therefore composed of two parts: a synthetic nucleic acid template that mimics the HIV target sequence in every way, except with a shuffled probe binding site, and a corresponding RPA nfo probe (probe chemistry is described in Piepenburg *et al.*[23]). To enable separate and specific detection of the HIV and IAC by lateral flow immunocapture, the HIV probe is labeled with digoxigenin while the IAC probe is labeled with 6-FAM.

We confirmed that the RPA assay sensitively detects as few as 10 copies of synthetic HIV or IAC DNA, with similar amplification efficiency and endpoint signal for each target, but virtually no cross-reactivity (Figure S1). In later experiments, we used synthetic DNA templates, where indicated, to demonstrate engineering concepts, as the assay is more sensitive to DNA. We also synthesized or extracted RNA templates to test the clinical viability of this assay, as HIV virions in plasma possess RNA genomes.

Competitive RPA Enables Software and Cell-Phone Quantification of HIV DNA Inputs That Vary ≥0.2-Fold (~0.1 $\log_{10}$) from IAC DNA Threshold

By co-amplifying a constant copy number of IAC with varying copy numbers of HIV, we found that the endpoint HIV signal fraction approximates the input HIV copy number fraction and can be used to identify the predominant target with high accuracy (Figure 2). 1000 copies of IAC DNA (representing the WHO VL threshold for a 1mL plasma sample) and varying copy numbers of HIV DNA (representing a sample with unknown VL) were added to RPA nfo reactions and run on lateral flow strips. We then quantified capture line signal intensities from scanned images and normalized them to the total (HIV + IAC)

signal. For all HIV inputs tested, the target with more copies at reaction initiation (input fraction > 0.5) produced a more intense capture line at endpoint (signal fraction > 0.5), even when the HIV input differed from the 1000-copy IAC threshold by just 200 copies (20%, corresponding to a difference of less than 0.1 $\log_{10}$). This implies that competitive RPA can be used to compare an HIV input to a certain threshold (represented by the IAC) with resolution comparable or superior to qPCR, but with much simpler instrumentation.

A similar analysis approach was conducted using cell phone photos processed by a custom MATLAB script. We took photos of the strips on a laboratory benchtop using an iPhone 11 camera and processed the images using a custom MATLAB script (see supplement for code). While the cell phone analysis slightly overestimated HIV relative to IAC (the average HIV signal fraction exceeds IAC signal fraction when HIV input = 800 copies DNA), the dominant signal at endpoint generally corresponded to the more abundant target at initiation. The slight overestimation of HIV relative to IAC may have occurred in cell phone photos due to non-uniform ambient lighting that could not be fully negated via background subtraction. Further development of cell phone image analysis algorithms, coupled with optical guides on lateral flow cassettes and real-time feedback via phone app to improve camera lighting, exposure, and focus, could improve the accuracy of this method and enable user self-testing[24].

We also observed that despite the correlation between HIV and IAC input and signal fractions, both signal fractions exhibited a systematic bias towards a value of 0.5 (in other words, the more abundant target was typically underestimated). We attribute this effect to the RPA nfo probe system, which does not directly produce signal upon binding to amplicons, but relies on enzymatic cleavage of bound probes. Any turnover in this process (i.e., ability of multiple probes to sequentially bind to one amplicon and get cleaved) to the point of saturation likely drives the endpoint HIV or IAC signal fractions to approximate the fraction of their respective probe concentrations (fixed to 0.5 for both probes), rather than the fraction of amplicons. Another potential reason for underestimation of the more abundant target is re-annealing of amplicons[25], which inhibits primer or probe binding and disproportionately affects the more abundant target. These effects have little impact on our goal to semi-quantitatively compare HIV to a clinical VL threshold, but would affect the accuracy of full quantification. While it should be possible to fully quantify a target using competitive RPA (as has been demonstrated using competitive SDA[15] or PCR[16]), additional development should be performed to counteract underestimation of the more abundant target. We suggest using an alternative probe chemistry that directly detects amplicons upon hybridization (e.g. molecular beacons[26] or Pleiades probes[27]), though care must be taken to ensure that the DNA-binding proteins used in RPA do not interfere with probe chemistry[28].

To improve quantification and determine statistical confidence in the assay results, we performed non-linear regression analysis on the data from each experiment to define the relationship between HIV input copy number and HIV signal fraction. The resulting sigmoidal curves resemble the plots of theoretical results, but essentially correct for systematic underestimation of the more abundant target by finding best-fit parameters for the baselines, slopes, and midpoints of each curve (see Table S2 for these parameters). Scatter of the data around each curve can then be used to generate a 95% prediction band,

which is the area around the curve that is expected to encompass 95% of future samples. For semi-quantitative applications, this analysis can effectively be used to estimate whether 95% of samples at a given HIV copy number will consistently produce an HIV signal fraction above or below a semi-quantitative diagnostic threshold. For example, the prediction bands for scanned image analysis of HIV inputs of 800 or 1200 copies slightly overlap the 0.5 signal fraction threshold (Figure 2, second plot from right), implying these inputs may occasionally be misdiagnosed with >5% frequency, but inputs of 600 or 1400 copies have prediction bands that do not overlap the 0.5 signal fraction threshold and should therefore be misdiagnosed with <5% frequency. For quantitative applications, this analysis may be used to interpolate unknown samples (the curve estimates the HIV copy number that produced a given HIV signal fraction, while a horizontal line that is drawn across the 95% prediction band at that signal fraction defines a 95% confidence interval for the input copy number). We believe this analysis is a powerful and convenient way to predict the performance of an assay and analyze its results, provided that it is validated across experiments and conditions in which the assay will be used.

Competitive RPA Enables Naked-Eye Quantification of HIV DNA Relative to Threshold

To demonstrate the feasibility of naked-eye analysis of these strips, we had 21 minimally trained volunteers interpret scanned strip images (Figure 3) that were previously analyzed via software. The volunteers' judgment agreed well with the ground truth (true input copy numbers of HIV and IAC) and with software analysis despite being blinded to both. They were able to identify a dominant capture line (HIV or IAC) for all HIV DNA inputs that deviated from the IAC threshold by an order of magnitude or more, and correctly identified the dominant capture line as that of the target with a higher input copy number. They therefore correctly classified all DNA reactions as representative of treatment success or treatment failure, except for the reactions with no HIV or IAC DNA (which they correctly classified as "inconclusive") or the strips with 1000 copies each of HIV and IAC DNA (which were too close to call for most volunteers). Only 4/504 calls (0.8%) in this experiment differed from the ground truth, all of which judged the HIV signal to be higher than the IAC for two reactions with 1000 copies each of HIV and IAC. While this "HIV=IAC" condition is a somewhat indeterminate case (it is possible through random sampling that these reactions did have a higher HIV input than IAC, or vice versa), these "incorrect" calls agreed with the software analysis in Figure 2, which found a slightly higher HIV signal than IAC for the strips in question. The volunteers who made these "incorrect" calls may therefore have been *more* sensitive to minute differences in signal than the other volunteers. Altogether, these results show that naked-eye-determined comparison of lateral flow line intensities agrees with software quantification and may be sufficient for test analysis at the point of care.

Competitive RPA Maintains Quantitative Behavior Regardless of IAC Threshold, Inhibitory Conditions, or Common HIV Mutations

We tested the limitations of the assay (Figure 4) with lower IAC thresholds (to simulate lower sample yield or volume, or a different choice of treatment failure threshold), a lower incubation temperature (to simulate amplification inhibition), or HIV templates with mutations relative to the primer and probe designs (to simulate the HIV genetic diversity

expected in clinical samples). More detailed information on the justification for and effects of changing these parameters can be found in the supplement (Figures S4-S6).

Lower IAC thresholds may occur when some yield is lost during sample preparation (assuming the IAC is added prior to sample preparation as an extraction control), when lower volumes of sample are collected, or may intentionally be built into the assay to meet a different definition of treatment failure (e.g. the 200c/mL threshold used by the CDC[7]). Although sensitivity was reduced with low IAC inputs (2/3 reactions with 50 copies IAC and 5 copies HIV failed) (Figure S4) the assay either maintained accurate quantification of HIV relative to IAC or failed to detect both targets (an inconclusive result, which is preferable to a false negative) (Figure 4, left). This demonstrates that the IAC input need not be a specific quantity for a given assay, but may be set to any threshold that is useful for the desired application.

The IAC further serves to protect the assay against amplification inhibition that may otherwise affect quantification. Temperature is a significant determinant of RPA reaction speed and sensitivity[4,23], and quantification methods that estimate input copy numbers based on liftoff time may be sensitive to temperature variations without proper controls. Also, while RPA is robust to many inhibitors, it can be adversely affected by background DNA at concentrations typical of fingerstick blood samples (though serum, which contains HIV virions and is commonly used in viral load tests, does not significantly inhibit RPA)[29,30]. While the optimal incubation temperature for this assay is 39°C[14], a POC test with minimal instrumentation may lack tight control of incubation temperature. We tested the function of this assay at 30°C to simulate a POC scenario with an imprecise heater, which also serves as a useful model system for any kind of reaction inhibition, such as that caused by background DNA. Although reactions at 30°C took longer to qualitatively detect 1000 copies of HIV DNA than at 39°C (Figure S5), the competitive assay (Figure 4, center) maintained accurate quantification of HIV relative to IAC due to the normalizing effect of the IAC. This demonstrates that errors in quantification are less likely to occur when a competitive IAC is used rather than a non-competitive IAC or external standards (which are commonly used for real-time PCR), as long as the cause of inhibition affects HIV and IAC amplification equally. However, we have noted the large variation of reactions with an HIV/IAC DNA input ratio of 1 in this experiment. We believe this variation is due to delayed mixing. Briefly, mixing ensures that amplification initiation and efficiency are consistent for HIV and IAC, but imperfect or delayed mixing may randomly favor one target over another. For this reason, a competitive assay procedure must ensure that proper mixing is achieved, particularly in low-resource settings. Further discussion on this point is in the Supporting Information (Figure S5).

However, mutations in the HIV template are a unique scenario in which HIV amplification could be adversely affected relative to that of the IAC and lead to an underestimate of VL, especially when variant HIV sequences exhibit mismatches to the primers or probe. We note that the qualitative version of this RPA assay has been shown to detect 51/56 sequences from a diverse panel of HIV variants in 3/3 replicate reactions, including one variant with 9 total mismatches to the primers and probe, although 1–4 mismatches are more common and the effect of any mismatch appears to depend on its location[14]. To assess the risk

that HIV mutations could affect the accuracy of quantification even if qualitative detection is maintained, we ran the competitive RPA assay using HIV templates with a subtype B consensus sequence (1 mismatch to the forward primer), subtype C consensus sequence (1 mismatch each to the reverse primer and probe), and a “Franken”-subtype sequence that we created to represent the combined mutations of all HIV-1 Group M subtype consensus sequences relative to the primers and probe (9 total mismatches to the primers and probe) (see Figure S6 for a sequence alignment). The assay maintained accuracy with the subtype B and C sequences, but in the case of the “Franken”-subtype, we observed no detection of HIV (unlike the aforementioned 9-mismatch variant[14]; we believe that differing locations of mutations caused this discrepancy), while the IAC was unaffected (Figure 4, right). We conclude that the competitive RPA assay is robust to common HIV mutations to a certain extent, but in rare cases with abundant mutations or mutations in locations that are critical to primer or probe function, a false negative for HIV treatment failure may result. We therefore urge careful *in silico* or clinical evaluation before using this assay in PWH cohorts who are expected to have high HIV sequence diversity, but we note that similar validation is needed for most HIV NATs regardless of the assay format. Fortunately, the geographical distribution of HIV-1 genomic diversity is well-documented, with hundreds of thousands of PWH sample sequences available from 116 countries from 1990 to 2015 (in general, diversity is low in India, Ethiopia, Southern Africa, and the United States, while diversity is high in Western Europe and Central Africa)[31]. With this knowledge, *in silico* screening of this assay against HIV genome alignments by country can be a useful tool to identify mutations to validate the assay against, or to confirm that the HIV genomic diversity of a PWH cohort meets a minimum desired prevalence of pre-validated sequences for assay compatibility.

One-Pot Competitive RT-RPA Enables Quantification of HIV RNA Relative to Threshold

To demonstrate the ability of this assay to quantify HIV RNA, as needed in a clinical VL test, we ran reactions with synthetic RNA targets (Figure 5) and analyzed them with the same survey or software approaches previously performed on DNA targets. Overall, the survey and software analyses agreed well with each other and with the ground truth. While the survey and software analysis both appeared to slightly underestimate HIV RNA relative to IAC RNA in the HIV=IAC condition (see the abundant ‘D’ responses in the survey where HIV=10^3, or the HIV signal fractions substantially lower than 0.5 in software analysis of the same strips), the agreement between the two analyses indicates that this underestimation is not due to errors in either analysis method. Given the tight accuracy of quantification previously observed with DNA targets, we believe that the HIV RNA target may have degraded slightly more than the IAC prior to RPA, although it is also possible that reverse transcription of the IAC target is more efficient (perhaps due to loss of secondary structure). We observed similar behavior when we tested the assay against HIV RNA extracted from clinical samples (Figure S7). Nevertheless, it appears that naked-eye and software analysis are both capable of distinguishing ≥10-fold ($\log_{10}$-scale) differences in HIV RNA copy number from the WHO treatment failure threshold. This may be sufficient for most VL tests, as PWH who discontinue ART typically experience a viral rebound with VL exceeding thresholds for treatment failure by an order of magnitude or more (in a prospective study, mean VL for 18 PWH exceeded 10^4 copies RNA/mL within 4 weeks of stopping ART[32]).

Conclusions

Competitive isothermal amplification is a powerful tool for quantification of nucleic acids and is useful for semi-quantitative HIV VL testing. The endpoint-measured lateral flow system enables naked-eye interpretation for most tests, while software and/or cell-phone mediated analysis can make a diagnosis when VL is too close to the treatment failure threshold for visual interpretation to be definitive. Furthermore, the competitive IAC controls for the variability of isothermal reactions and confers robustness to several potential complications, including low sample preparation yield, reaction inhibition, and common HIV mutants. Competitive IACs have been used for HIV VL quantification before[15,16], and a semi-quantitative lateral-flow-based VL test (SAMBA semi-Q) has been described[33], but the competitive RPA assay described herein is the first (to our knowledge) to combine these technologies into a low-resource workflow.

A clinical adaptation of this assay should focus on development of a kit to address other POC priorities, such as ready-to-use shelf-stable reagents, low-resource sample preparation, and prevention of amplicon contamination. Although lyophilized RPA reaction pellets are recommended to be stored at −20°C, one study suggests that they remain viable at 25°C for three months or at 45°C for three weeks[5], which simplifies distribution and storage in low-resource settings (furthermore, the IAC could indicate reaction failure due to expired reagents). A more important concern for reagent storage is ease of use; ideally, all oligos should be stored with the lyophilized pellet to reduce assay setup complexity[34,35], and any liquid reagents should be combined into a single, small volume that is easy to add to the pellet (e.g. with a single-use exact volume transfer pipette). We have observed favorable performance and user feedback with a similar workflow conducted by non-trained 1st-time users or healthcare workers for HIV[34,36] or SARS-CoV-2 assays[37]. These changes have the added benefit of minimizing reagent volume, which allows for a larger sample input volume. Sample preparation must also be addressed in a clinical implementation; a blood sample for VL testing must first be collected, filtered or otherwise processed to remove cellular components, and purified to remove ribonucleases and other inhibitors and concentrate viral RNA[12]. We did not address sample preparation in this work, but paper-based methods for processing viral RNA from human specimens have been described[38,39]. A more sensitive RT-RPA assay[40,41] may also be desired if a PWH cohort is expected to have lower VLs or if the desired sampling method is a fingerstick. Finally, containment of amplicons is essential to prevent contamination of future tests carried out in the same location. This can be achieved procedurally through separation of pre- and post-amplification workspaces in clinics, for example, but for self-testing, a sealed lateral flow cartridge (e.g., U-Star Disposable Nucleic Acid Lateral Flow Detection Units) may be ideal.

The assay chemistry described here is aimed at a specific application for HIV VL testing, but the concept and utility of a competitive IAC may be generalized to many isothermal amplification systems and applications. Indeed, although RPA nfo is a discontinued product at the time of writing, we have developed a fluorescence-based version of this assay using the RPA exo kit with similar semi-quantitative behavior (not shown). We also suggest that the nfo kit chemistry could be replicated by adding *E. coli* endonuclease IV to the basic RPA chemistry, as described in Piepenburg *et al.*[23]. Competitive amplification may be

used in practically any chemistry with multiplexable detection methods[15,42]. Loop-mediated isothermal amplification (LAMP), for example, is another multiplexable chemistry used for POC diagnostics[43], and a direct RT-LAMP assay for HIV RNA detection in whole blood has been described[44]. Adaptation of such assays with demonstrated robustness to include a competitive IAC and a lateral flow readout should be relatively straightforward, although the barriers to POC implementation described previously still apply to virtually any NAT. Further innovations in the assay chemistry, such as direct measurement of amplicons with a hybridization-based probe system, may enable full quantification when desired for HIV VL testing or other POC applications.

Supplementary Material

Refer to Web version on PubMed Central for supplementary material.

Acknowledgments

We thank other Lutz Lab members (Amy Oreskovic, Daniel Leon, Shane Gilligan-Steinberg, and Robert Atkinson), members of the Frenkel Lab (Ingrid Beck, Ceejay Boyce, and Jackson Wallner), and members of the Yager Lab (Paul Yager, Sujatha Kumar, and Erin Heiniger) for their technical advice and helpful discussion. We thank Rongyu Zhang for preliminary development of lateral flow assays. We thank Paul Drain for advice pertaining to the clinical applications of this assay in HIV viral load monitoring. This work was supported by NIH/NIAID research grants R61AI140460 and R01AI145486. I.T.H. was supported in part by the National Institute of General Medical Sciences of the National Institutes of Health under Award Number T32GM008268.

Supporting Information

Additional experimental methods, results, and discussion, including oligo and template sequences, regression analysis parameters, lateral flow strip images, survey design, oligo-template sequence alignment, and MATLAB script.

REFERENCES

(1). Niemz A; Ferguson TM; Boyle DS Point-of-Care Nucleic Acid Testing for Infectious Diseases. Trends Biotechnol. 2011, 29 (5), 240–250. 10.1016/j.tibtech.2011.01.007. [PubMed: 21377748]

(2). Obande GA; Singh KKB Current and Future Perspectives on Isothermal Nucleic Acid Amplification Technologies for Diagnosing Infections. Infect. Drug Resist. 2020, 13, 483. 10.2147/IDR.S217571.

(3). Jansson L; Hedman J Challenging the Proposed Causes of the PCR Plateau Phase. Biomol. Detect. Quantif. 2019, 17, 100082. 10.1016/J.BDQ.2019.100082.

(4). Lillis L; Lehman D; Singhal MC; Cantera J; Singleton J; Labarre P; Toyama A; Piepenburg O; Parker M; Wood R; Overbaugh J; Boyle DS Non-Instrumented Incubation of a Recombinase Polymerase Amplification Assay for the Rapid and Sensitive Detection of Proviral HIV-1 DNA. PLoS One 2014, 9 (9), e108189. 10.1371/journal.pone.0108189.

(5). Lillis L; Siverson J; Lee A; Cantera J; Parker M; Piepenburg O; Lehman DA; Boyle DS Factors Influencing Recombinase Polymerase Amplification (RPA) Assay Outcomes at Point of Care. 2016, 30 (2). 10.1016/j.mcp.2016.01.009.

(6). World Health Organization. Consolidated Guidelines on the Use of Antiretroviral Drugs for Treating and Preventing HIV Infection: Recommendations for a Public Health Approach, 2nd ed.; World Health Organization: Geneva, 2016.

(7). Centers for Disease Control and Prevention. HIV Treatment as Prevention https://www.cdc.gov/hiv/risk/art/index.html (accessed Aug 23, 2021).

(8). Institute for Health Metrics and Evaluation. GBD Results Tool http://ghdx.healthdata.org/gbd-results-tool (accessed Aug 20, 2021).

(9). Mazzola LT; Pérez-Casas C HIV/AIDS Diagnostics Technology Landscape, 5th Edition; Geneva, Switzerland, 2015.

(10). UNAIDS. Ending AIDS: Progress towards the 90–90–90 Targets; 2017.

(11). UNAIDS. UNAIDS DATA 2017; 2017.

(12). Drain PK; Dorward J; Bender A; Lillis L; Marinucci F; Sacks J; Bershteyn A; Boyle DS; Posner JD; Garrett N Point-of-Care HIV Viral Load Testing: An Essential Tool for a Sustainable Global HIV/AIDS Response. Clin. Microbiol. Rev. 2019, 32 (3), e00097–18. 10.1128/CMR.00097-18.

(13). Crannell ZA; Rohrman B; Richards-Kortum R Quantification of HIV-1 DNA Using Real-Time Recombinase Polymerase Amplification. Anal. Chem. 2014, 86 (12), 5615–5619. 10.1021/ac5011298. [PubMed: 24873435]

(14). Boyle DS; Lehman DA; Lillis L; Peterson D; Singhal M; Armes N; Parker M; Piepenburg O; Overbaugh J Rapid Detection of HIV-1 Proviral DNA for Early Infant Diagnosis Using Recombinase Polymerase Amplification. MBio 2013, 4 (2), e00135–13. 10.1128/mBio.00135-13.

(15). Nycz CM; Dean CH; Haaland PD; Spargo CA; Walker GT Quantitative Reverse Transcription Strand Displacement Amplification: Quantitation of Nucleic Acids Using an Isothermal Amplification Technique. Anal. Biochem. 1998, 259 (2), 226–234. 10.1006/ABIO.1998.2641. [PubMed: 9618201]

(16). Piatak M; Saag M; Yang L; Clark S; Kappes J; Luk K; Hahn B; Shaw G; Lifson J High Levels of HIV-1 in Plasma during All Stages of Infection Determined by Competitive PCR. Science (80-.). 1993, 259 (5102), 1749–1754. 10.1126/science.8096089.

(17). Los Alamos National Laboratory. HIV Sequence Database https://www.hiv.lanl.gov/content/sequence/HIV/mainpage.html (accessed May 8, 2018).

(18). Mathworks. MATLAB R2019a. The Mathworks, Inc.: Natick, Massachusetts 2019.

(19). d'Agostino RB Tests for Normal Distribution. In Goodness-Of-Fit Techniques; d'Agostino RB, Stephens MA, Eds.; Marcel Dekker: New York, NY, 1986.

(20). Schneider CA; Rasband WS; Eliceiri KW NIH Image to ImageJ: 25 Years of Image Analysis. Nat. Methods 2012, 9 (7), 675. 10.1038/NMETH.2089.

(21). Moody C; Newell H; Viljoen H A Mathematical Model of Recombinase Polymerase Amplification under Continuously Stirred Conditions. Biochem. Eng. J. 2016, 112, 193–201. 10.1016/J.BEJ.2016.04.017.

(22). Arezi B; Xing W; Sorge JA; Hogrefe HH Amplification Efficiency of Thermostable DNA Polymerases. Anal. Biochem. 2003, 321 (2), 226–235. 10.1016/S0003-2697(03)00465-2. [PubMed: 14511688]

(23). Piepenburg O; Williams CH; Stemple DL; Armes NA DNA Detection Using Recombination Proteins. PLoS Biol. 2006, 4 (7), e204. 10.1371/journal.pbio.0040204. [PubMed: 16756388]

(24). Park C; Ngo H; Lavitt LR; Karuri V; Bhatt S; Lubell-Doughtie P; Shankar AH; Ndwiga L; Osoti V; Wambua JK; Bejon P; Ochola-Oyier LI; Chilver M; Stocks N; Lyon V; Lutz BR; Thompson M; Mariakakis A; Patel S The Design and Evaluation of a Mobile System for Rapid Diagnostic Test Interpretation. Proc. ACM Interactive, Mobile, Wearable Ubiquitous Technol. 2021, 5 (1), 1–26.

(25). Mathieu-Daudé F; Welsh J; Vogt T; McClelland M DNA Rehybridization During PCR: The 'C o t Effect' and Its Consequences. Nucleic Acids Res. 1996, 24 (11), 2080–2086. 10.1093/NAR/24.11.2080. [PubMed: 8668539]

(26). Tyagi S; Kramer FR Molecular Beacons: Probes That Fluoresce upon Hybridization. Nat. Biotechnol. 1996, 14 (3), 303–308. 10.1038/nbt0396-303. [PubMed: 9630890]

(27). Lukhtanov EA; Lokhov SG; Gorn VV; Podyminogin MA; Mahoney W Novel DNA Probes with Low Background and High Hybridization-Triggered Fluorescence. Nucleic Acids Res. 2007, 35 (5), e30. 10.1093/nar/gkl1136. [PubMed: 17259212]

(28). Wang L; Yang CJ; Medley CD; Benner SA; Tan W Locked Nucleic Acid Molecular Beacons. J. Am. Chem. Soc. 2005, 127 (45), 15664–15665. 10.1021/JA052498G. [PubMed: 16277483]

(29). Kersting S; Rausch V; Bier FF; von Nickisch-Rosenegk M Rapid Detection of Plasmodium Falciparum with Isothermal Recombinase Polymerase Amplification and Lateral Flow Analysis. Malar. J. 2014, 13 (1), 99. 10.1186/1475-2875-13-99. [PubMed: 24629133]

(30). Rohrman B; Richards-Kortum R Inhibition of Recombinase Polymerase Amplification by Background DNA: A Lateral Flow-Based Method for Enriching Target DNA. Anal. Chem. 2015, 87 (3), 1963–1967. 10.1021/ac504365v. [PubMed: 25560368]

(31). Hemelaar J; Loganathan S; Elangovan R; Yun J; Dickson-Tetteh L; Kirtley S; WHO-UNAIDS Network for HIV Isolation and Characterization. Country Level Diversity of the HIV-1 Pandemic between 1990 and 2015. J. Virol. 2020, 95 (2), e01580–20. 10.1128/JVI.01580-20.

(32). Davey RT; Bhat N; Yoder C; Chun T-W; Metcalf JA; Dewar R; Natarajan V; Lempicki RA; Adelsberger JW; Miller KD; Kovacs JA; Polis MA; Walker RE; Falloon J; Masur H; Gee D; Baseler M; Dimitrov DS; Fauci AS; Lane HC HIV-1 and T Cell Dynamics after Interruption of Highly Active Antiretroviral Therapy (HAART) in Patients with a History of Sustained Viral Suppression. Proc. Natl. Acad. Sci. 1999, 96 (26), 15109–15114. 10.1073/PNAS.96.26.15109.

(33). Ritchie AV; Ushiro-Lumb I; Edemaga D; Joshi HA; De Ruiter A; Szumilin E; Jendrulek I; McGuire M; Goel N; Sharma PI; Allain JP; Lee HH SAMBA HIV Semiquantitative Test, a New Point-of-Care Viral-Load-Monitoring Assay for Resource-Limited Settings. J. Clin. Microbiol. 2014, 52 (9), 3377–3383. 10.1128/JCM.00593-14. [PubMed: 25031444]

(34). Panpradist N; Beck IA; Vrana J; Higa N; McIntyre D; Ruth PS; So I; Kline EC; Kanthula R; Wong-On-Wing A; Lim J; Ko D; Milne R; Rossouw T; Feucht UD; Chung M; Jourdain G; Ngo-Giang-Huong N; Laomanit L; Soria J; Lai J; Klavins ED; Frenkel LM; Lutz BR OLA-Simple: A Software-Guided HIV-1 Drug Resistance Test for Low-Resource Laboratories. EBioMedicine 2019, 50, 34–44. 10.1016/j.ebiom.2019.11.002. [PubMed: 31767540]

(35). Panpradist N; Wang Q; Ruth PS; Kotnik JH; Oreskovic AK; Miller A; Stewart SWA; Vrana J; Han PD; Beck IA; Starita LM; Frenkel LM; Lutz BR Simpler and Faster Covid-19 Testing: Strategies to Streamline SARS-CoV-2 Molecular Assays. EBioMedicine 2021, 64, 103236. 10.1016/J.EBIOM.2021.103236.

(36). Vrana JD; Panpradist N; Higa N; Ko D; Ruth P; Kanthula R; Lai JJ; Yang Y; Sakr SR; Chohan B; Chung MH; Frenkel LM; Lutz BR; Klavins E; Beck IA; Klavins Biosystems E Implementation of an Interactive Mobile Application to Pilot a Rapid Assay to Detect HIV Drug Resistance Mutations in Kenya. medRxiv 2021, 2021.05.06.21256654. 10.1101/2021.05.06.21256654.

(37). Panpradist N; Kline E; Atkinson RG; Roller M; Wang Q; Hull IT; Kotnik JH; Oreskovic AK; Bennett C; Leon D; Lyon V; Gilligan-Steinberg SD; Han PD; Drain PK; Starita LM; Thompson MJ; Lutz BR Harmony COVID-19: A Ready-to-Use Kit, Low-Cost Detector, and Smartphone App for Point-of-Care SARS-CoV-2 RNA Detection. Sci. Adv. 2021, (in press).

(38). Rodriguez NM; Linnes JC; Fan A; Ellenson CK; Pollock NR; Klapperich CM Paper-Based RNA Extraction, in Situ Isothermal Amplification, and Lateral Flow Detection for Low-Cost, Rapid Diagnosis of Influenza A (H1N1) from Clinical Specimens. Anal. Chem. 2015, 87 (15), 7872–7879. 10.1021/ACS.ANALCHEM.5B01594. [PubMed: 26125635]

(39). Phillips EA; Moehling TJ; Ejendal KFK; Hoilett OS; Byers KM; Basing LA; Jankowski LA; Bennett JB; Lin LK; Stanciu LA; Linnes JC Microfluidic Rapid and Autonomous Analytical Device (MicroRAAD) to Detect HIV from Whole Blood Samples. Lab Chip 2019, 19 (20), 3375–3386. 10.1039/C9LC00506D. [PubMed: 31539001]

(40). Lillis L; Lehman DA; Siverson JB; Weis J; Cantera J; Parker M; Piepenburg O; Overbaugh J; Boyle DS Cross-Subtype Detection of HIV-1 Using Reverse Transcription and Recombinase Polymerase Amplification. J. Virol. Methods 2016, 230, 28–35. [PubMed: 26821087]

(41). Qian J; Boswell SA; Chidley C; Lu Z; Pettit ME; Gaudio BL; Fajnzylber JM; Ingram RT; Ward RH; Li JZ; Springer M An Enhanced Isothermal Amplification Assay for Viral Detection. Nat. Commun. 2020, 11 (1), 5920. 10.1038/s41467-020-19258-y. [PubMed: 33219228]

(42). Piatak M; Luk KC; Williams B; Lifson JD Quantitative Competitive Polymerase Chain Reaction for Accurate Quantitation of HIV DNA and RNA Species. Biotechniques 1993, 14 (1), 70–81. [PubMed: 8424881]

(43). Wong YP; Othman S; Lau YL; Radu S; Chee HY Loop-Mediated Isothermal Amplification (LAMP): A Versatile Technique for Detection of Micro-Organisms. J. Appl. Microbiol. 2018, 124 (3), 626–643. 10.1111/JAM.13647. [PubMed: 29165905]

(44). Curtis KA; Rudolph DL; Owen SM Rapid Detection of HIV-1 by Reverse-Transcription, Loop-Mediated Isothermal Amplification (RT-LAMP). J. Virol. Methods 2008, 151 (2), 264–270. 10.1016/j.jviromet.2008.04.011. [PubMed: 18524393]

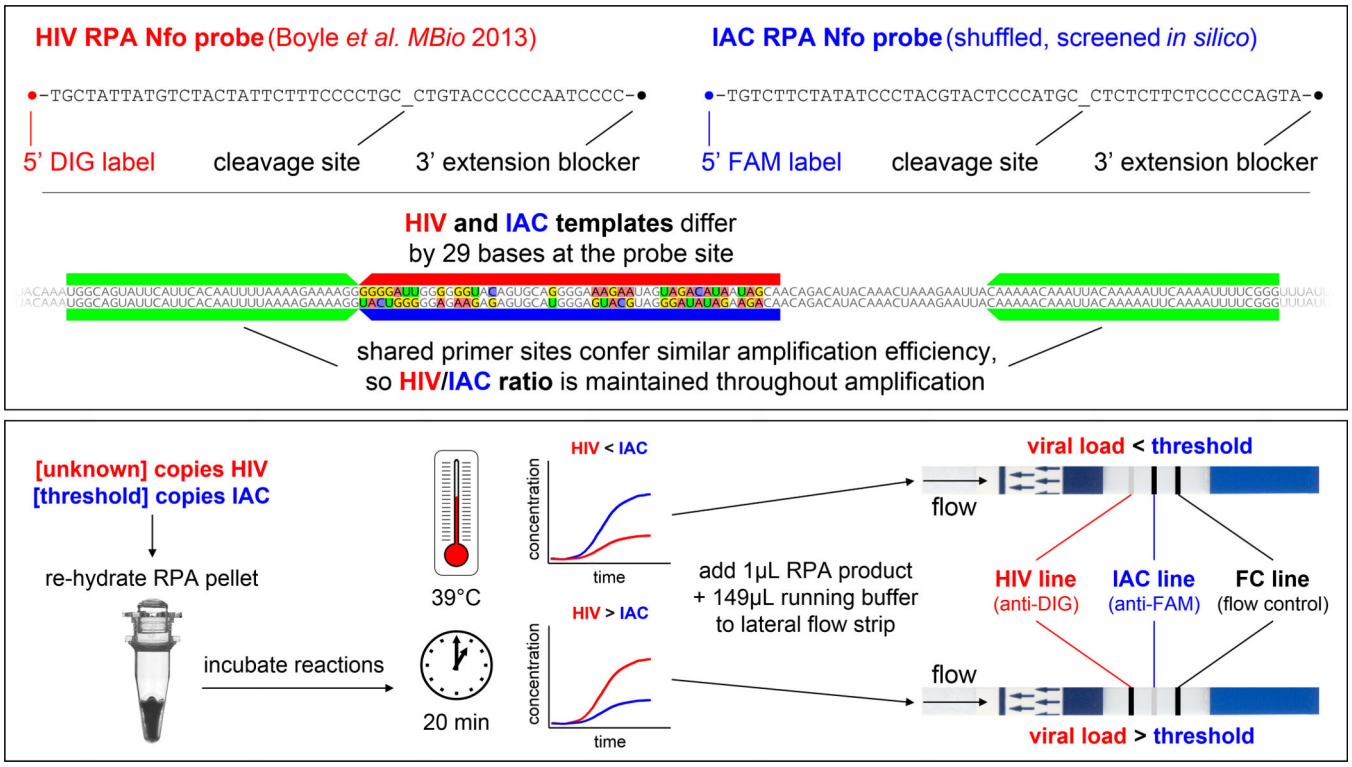

Figure 1. Competitive IAC design and concept.

(TOP) Sequences for HIV and IAC probes and synthetic templates. HIV probe sequence is unchanged from Boyle *et al.*[14] but has been modified to use digoxigenin (DIG) as an antigenic label. IAC probe sequence contains same base content as HIV probe but with shuffled sequence and a FAM antigenic label. (BOTTOM) Conceptual workflow for competitive RPA assay, with mock data demonstrating outcomes with HIV input below or above the VL threshold represented by the IAC. Because the HIV and IAC targets should amplify with similar efficiency, the endpoint HIV/IAC signal ratio should correspond to the input HIV/IAC ratio. (Note that RPA products flow from left to right in this depiction; the blue arrows on strips are physical stickers to indicate correct end down for placement of strips in sample wells).

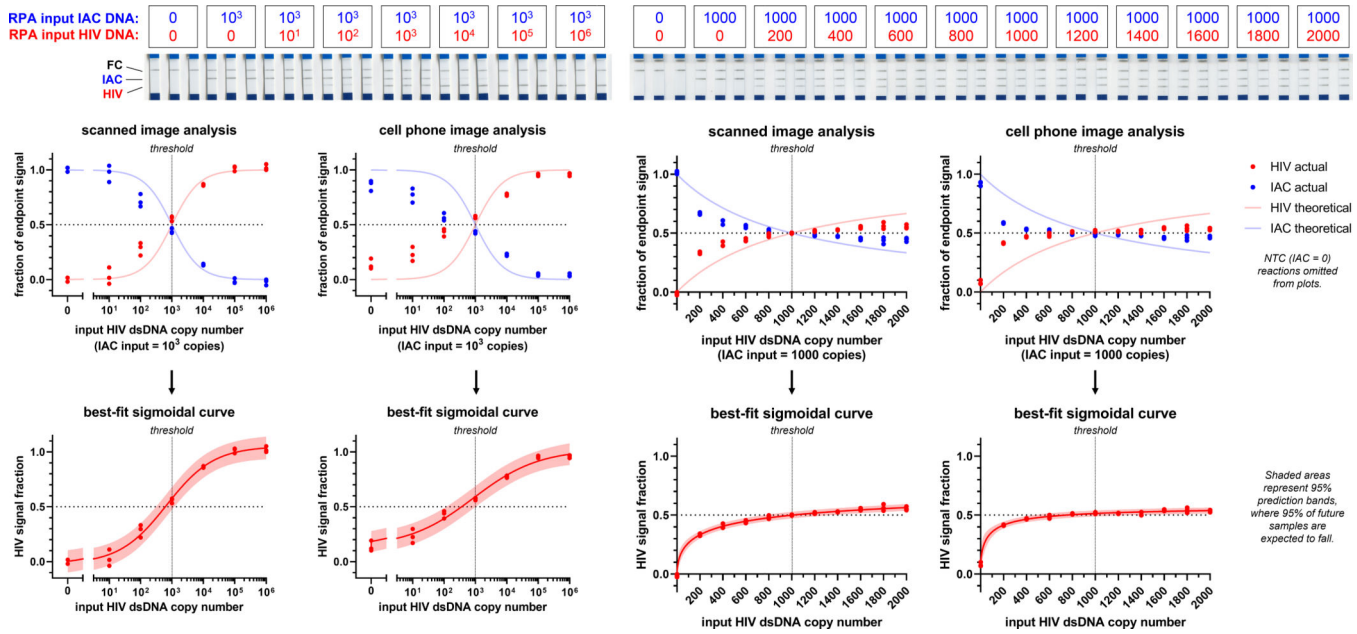

Figure 2. Competitive RPA results analyzed by software.

RPA reactions were run with 1000 copies IAC DNA and varying copy numbers of HIV DNA, then wicked through lateral flow strips for endpoint signal analysis. (TOP) Scanned images of lateral flow strips. (CENTER) Analysis of lateral flow strips using scanned images with ImageStudio Lite software or cell phone photos with a custom MATLAB script. Dots represent actual assay results (endpoint HIV or IAC signal divided by the sum of these signals) (N=3), while lines represent the theoretical or expected results (input HIV or IAC copy number divided by the sum of these copy numbers). (BOTTOM) Sigmoidal curve fit to assay results using non-linear regression analysis. Dots represent actual assay results (N=3). Lines represent a four-parameter logistic equation fit to the data in each plot. Shaded areas represent 95% prediction bands, where 95% of future samples are expected to fall.

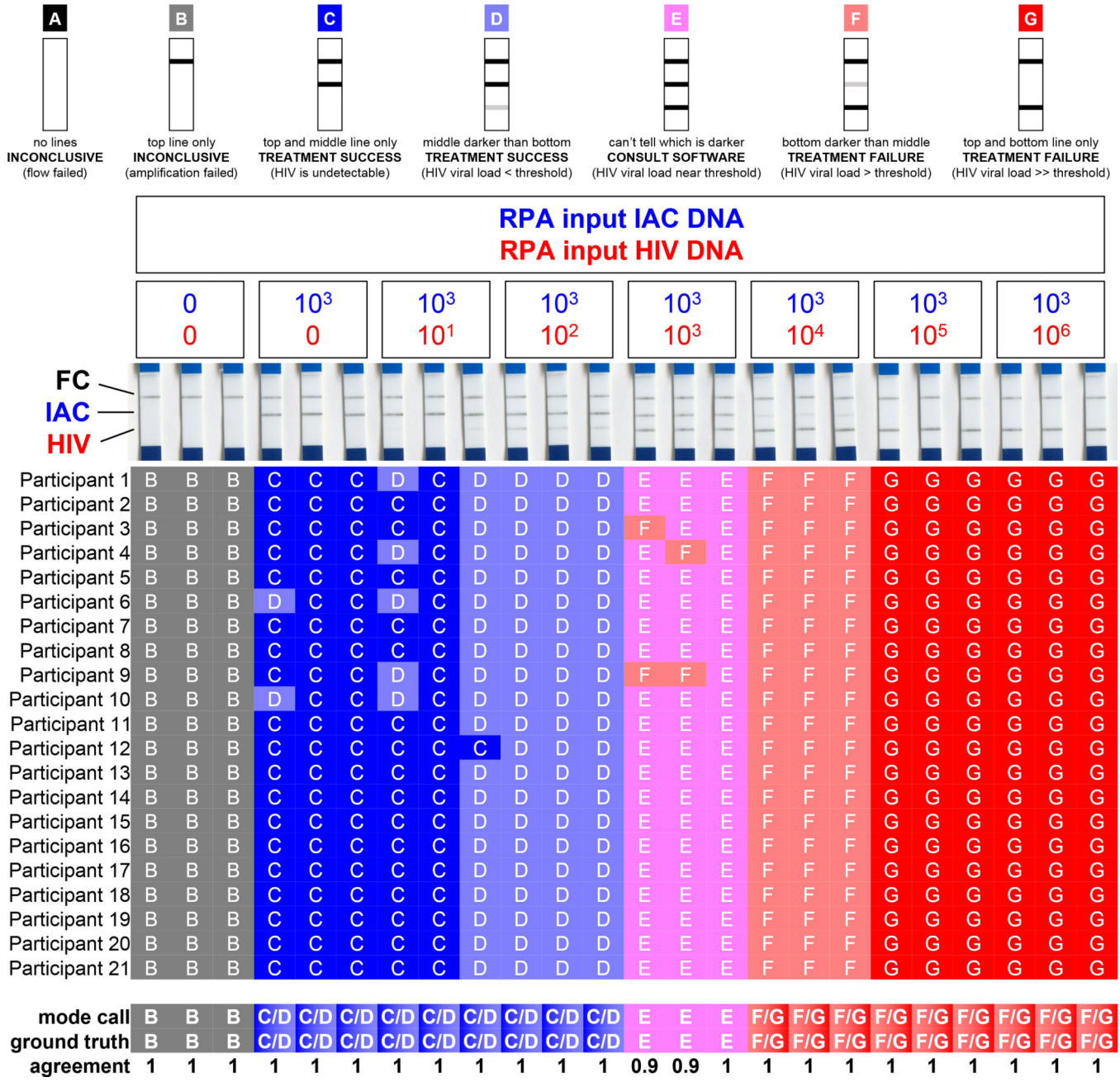

Figure 3. Competitive RPA results analyzed by naked eye survey.

Survey participants classified lateral flow strip results according to options in the schematic (TOP) for RPA reactions run with DNA targets. Individual and mode responses for each strip are displayed below strip images (CENTER) in a table (BOTTOM). Options C and D suggest successful HIV treatment under current WHO guidance and are thus combined in calculations, as are options F and G, which both represent treatment failure.

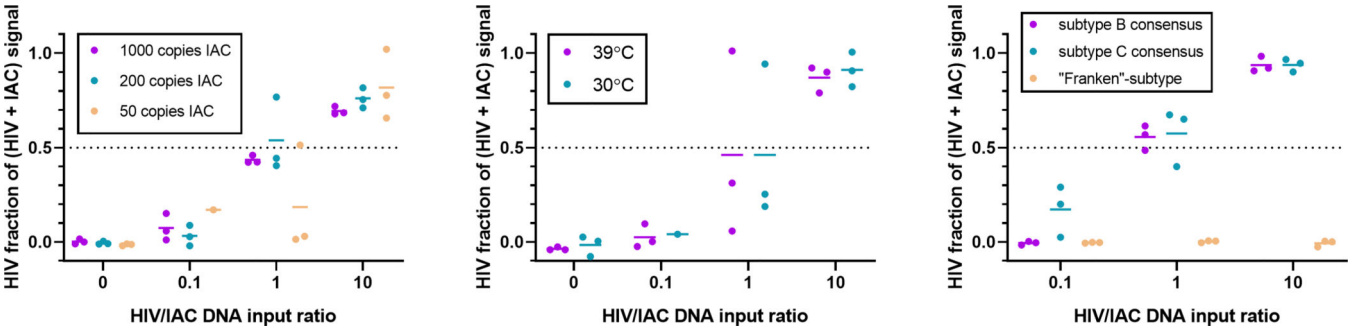

Figure 4. Competitive RPA assay results in response to changes in IAC copy number, incubation temperature, or HIV sequence.

RPA reactions were run with 1000 copies IAC DNA (unless otherwise specified) and varying ratios of HIV DNA relative to IAC, then wicked through lateral flow strips for endpoint signal analysis via scanner and ImageStudio Lite. Dots represent replicate assays while horizontal lines represent sample means (N=3). Failed reactions are omitted from analysis; see Figure S4 and Figure S5 for discussion. (LEFT) Competitive RPA assay with lower IAC thresholds (and proportional changes in HIV input) to simulate sample loss, lower sample volume, or lower thresholds for treatment failure. (CENTER) Competitive RPA assay at lower temperature to simulate reaction inhibition. (RIGHT) Competitive RPA with HIV template sequences based on subtypes of HIV-1 Group M to simulate mutations relative to primer and probe designs.

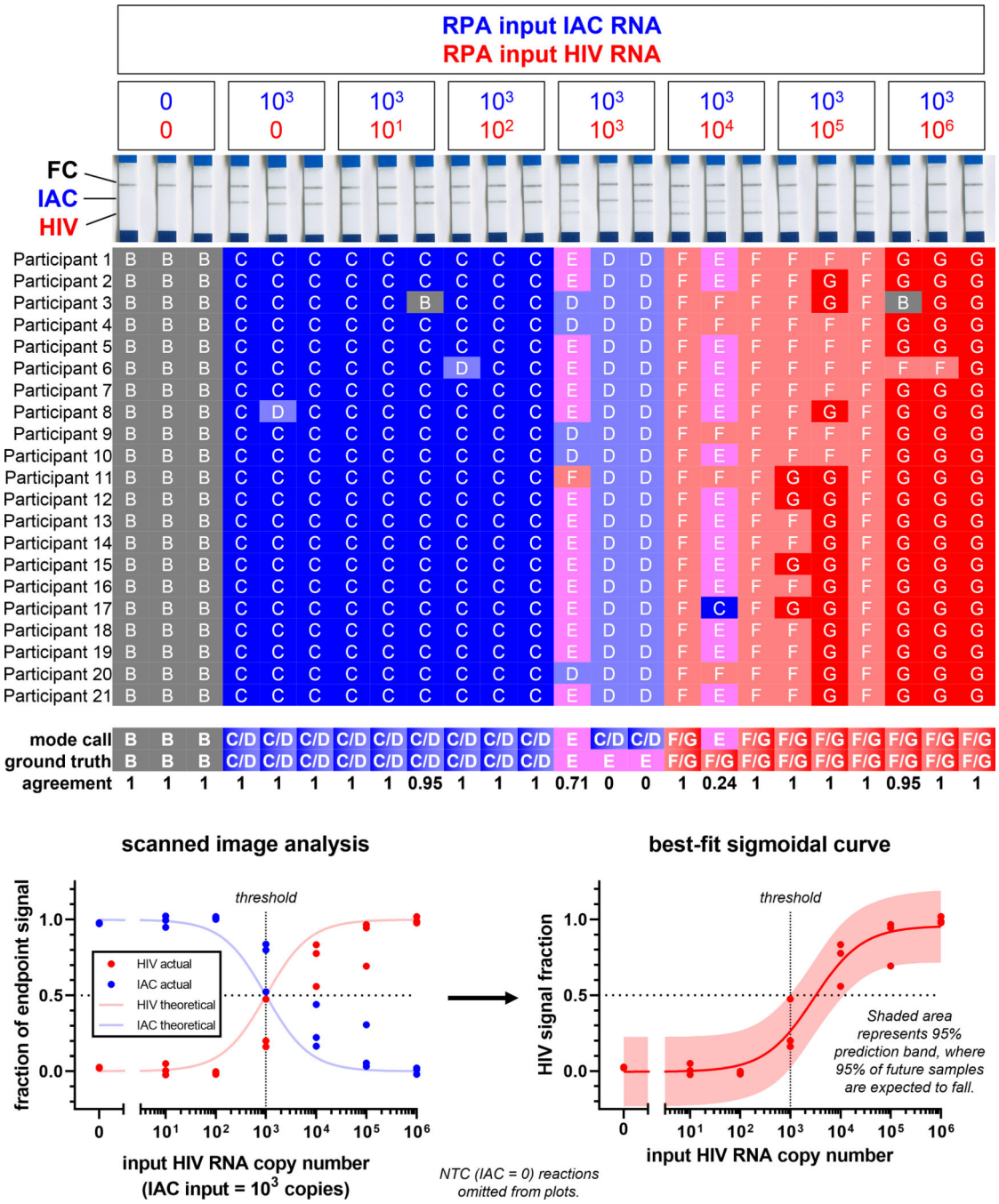

Figure 5. Competitive RT-RPA results analyzed by naked eye survey and by software.

RT-RPA reactions were run with 1000 copies IAC RNA and varying copy numbers of HIV RNA, then wicked through lateral flow strips for endpoint signal analysis. (TOP) Images of lateral flow strips. (CENTER) Survey responses for naked-eye analysis of each strip. (BOTTOM LEFT) Software analysis of strips via scanner and ImageStudio Lite. Dots represent actual assay results (endpoint HIV or IAC signal divided by the sum of these signals) (N=3), while lines represent the theoretical or expected results. (BOTTOM RIGHT) Sigmoidal curve fit to assay results using non-linear regression analysis. Dots represent

actual assay results (N=3). Lines represent a four-parameter logistic equation fit to the data in each plot. Shaded areas represent 95% prediction bands.